mathematics

Article

Stochastic Analysis of Nonlinear Cancer Disease Model through Virotherapy and Computational Methods

Ali Raza [1,*] **, Jan Awrejcewicz** [2] **, Muhammad Rafiq** [3] **, Nauman Ahmed** [4] **and Muhammad Mohsin** [5]

1   Department of Mathematics, Govt. Maulana Zafar Ali Khan Graduate College Wazirabad,
    Punjab Higher Education Department (PHED), Lahore 54000, Pakistan
2   Department of Automation, Biomechanics and Mechatronics, Lodz University of Technology,
    1/15 Stefanowskiego St., 90-924 Lodz, Poland; jan.awrejcewicz@p.lodz.pl
3   Department of Mathematics, Faculty of Sciences, University of Central Punjab, Lahore 54000, Pakistan;
    m.rafiq@ucp.edu.pk
4   Department of Mathematics and Statistics, The University of Lahore, Lahore 54590, Pakistan;
    nauman.ahmd01@gmail.com
5   Department of Mathematics, Chemnitz University of Technology, 09111 Chemnitz, Germany;
    muhammadmohsincheema@gmail.com
*   Correspondence: 160865@students.au.edu.pk

Abstract: Cancer is a common term for many diseases that can affect anybody. A worldwide leading cause of death is cancer, according to the World Health Organization (WHO) report. In 2020, ten million people died from cancer. This model identifies the interaction of cancer cells, viral therapy, and immune response. In this model, the cell population has four parts, namely uninfected cells (x), infected cells (y), virus-free cells (v), and immune cells (z). This study presents the analysis of the stochastic cancer virotherapy model in the cell population dynamics. The model results have restored the properties of the biological problem, such as dynamical consistency, positivity, and boundedness, which are the considerable requirements of the models in these fields. The existing computational methods, such as the Euler Maruyama, Stochastic Euler, and Stochastic Runge Kutta, fail to restore the abovementioned properties. The proposed stochastic nonstandard finite difference method is efficient, cost-effective, and accommodates all the desired feasible properties. The existing standard stochastic methods converge conditionally or diverge in the long run. The solution by the nonstandard finite difference method is stable and convergent over all time steps.

Keywords: cancer model; stochastic differential equations; computational methods; stability analysis

1. Introduction

Cancer is a family of diseases associated with developing abnormal cells to seize or transmit to other parts of one's body. Cancer is the rapid emergence of abnormal cells which arise outside their normal limits, and it may occupy the linked parts of the body and transfer to the tissues afterward. Virotherapy is the treatment of cancer that detects or destroys cancer cells during the process, and healthy cells are not harmed. Tuwairqi et al. presented the qualitative analysis of cancer cells in the cell population [1]. In 2011, Crivelli et al. presented the cell dynamics with the recommendation of the control strategies [2]. In 2020, Nouni et al. analyzed the tumor cells' dynamics for the immune response of a virological model for cancer therapy [3]. Storey et al. developed a deterministic model for treating a tumor via oncolytic treatment [4]. Abernathy et al. investigated the dynamics of the cell population, including interactions between infected and uninfected brain tumor cells [5]. Matos et al. studied the new approaches for treating cancer-like infections [6]. Makaryan et al. analyzed the awareness strategies within immune cell actions and biological therapy techniques [7]. Malinzi et al. presented the wave propagation model for dynamics of chemo/virotherapy cancer [8]. Bajzer et al. developed a co-infection dynamic of the tumor

with measles in the human body [9]. Timalsina et al. developed computational techniques to model tumor virotherapy in the cell population [10]. Rommeifanger et al. developed a melanoma tumor model in the cell dynamics and performed its qualitative analysis [11]. Wares et al. established a mathematical model for cell-cycle-specific cancer virotherapy [2]. Liu et al. launched a comparison analysis of a deterministic and stochastic model for tumor-immune responses to chemotherapy [12]. Eftimie et al. investigated the complex dynamics of cell populations with well-known epidemiology techniques [13]. Santiago et al. presented the optimal control interventions [14]. Kim et al. established the hybrid analysis of cancer in the cell population [15]. Berg et al. introduced multidimensional modeling of oncolytic tumor virotherapy [16]. Some notable models related to cervical cancer and many more are presented in References [17–23]. The well-known methods in the sense of stochastic are presented in References [24,25]. This work aimed to understand the complex interplay among tumor cells, oncolytic viruses, and immune response. Thus, a dynamical analysis was employed to investigate the optimal therapeutic strategies for cancer remission. Stochastic analysis of the cancer disease is more realistic, practical, accurate, and close to nature. The stochastic differential equations have no analytic solutions, due to the non-differentiable term of Brownian motion. Thus, there is a need for computational methods to solve the said problems; furthermore, our focus is on those methods that restore the model's dynamical properties. That is why we moved to construct the nonstandard finite difference method in the sense of stochastic. The rest of the paper is organized based on the following sections: In Section 2, the deterministic cancer model's formulation has fundamental properties. Sections 3 and 4 deal with the stochastic model's transition probabilities, positivity, boundedness and implementation methods, convergence, and comparative analysis. Finally, the conclusion is presented in Section 5.

2. Deterministic Formulation

For any time, the states of the model are described as follows: $x(t)$ represents the uninfected cancer cells, $y(t)$ denotes the infected cancer cells, $v(t)$ gives the virus-free cells, and $z(t)$ shows the immune cells. Furthermore, the incoming and outgoing ratios are defined as λ, which is the growth rate of cells; C, which is the carrying capacity; d, which represents the death rate of cells that die due to natural causes or with infection; β, which is the rate of the oncolytic virus on cancer cells; δ, which is the rate of infected cells; b, which is the rate at which new version particles are released with burst size; and γ, which is the rate of decay of free virus-cell. Other ratios are defined as follows: α is the rate of uninfected cells due to immunity of the body, μ is the rate of infected cells due to weak immunity, k is the rate of elimination at which cancer cells become immune, h_2 is the rate of stimulation of uninfected cells by immunity, h_1 is the response rate at which infected cells become immuned, and ρ is the rate of decay of immune cells. The systematic flow of cancer disease is presented in Figure 1.
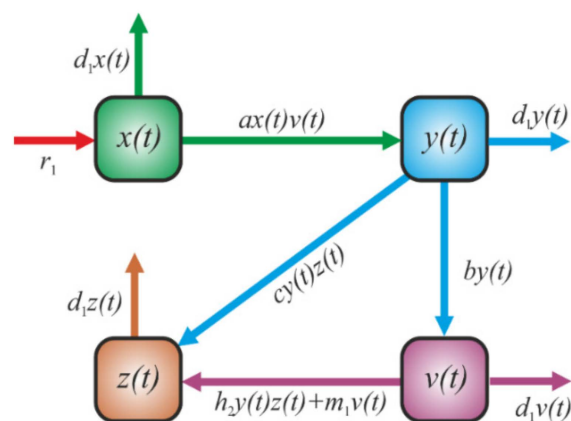

Figure 1. Flow map for the dynamics of the cancer epidemic model.

The nonlinear ordinary differential equations by using the law of mass action are as follows:

$$x'(t) = r_1 - axv - d_1 x, \ t \geq 0, \tag{1}$$

$$y'(t) = axv - cyz - d_1 y - by, \ t \geq 0, \tag{2}$$

$$v'(t) = by - h_2 yz - d_1 v - m_1 v, \ t \geq 0 \tag{3}$$

$$z'(t) = cyz + h_2 yz - d_1 z + m_1 v, \ t \geq 0 \tag{4}$$

with nonnegative (initial) conditions $x_0 = x(0) \geq 0, y_0 = y(0) \geq 0, v_0 = v(0) \geq 0$, $z_0 = z(0) \geq 0$ and $x + y + v + z = 1$.

2.1. Analysis of Model

In this section, we define the feasible region of the system (1)–(4) as follows:
$\Psi = \{(x(t), y(t), v(t), z(t)) \varepsilon \ R\_ +\hat{}4 : N(t) \leq r\_1/d\_1, \ x\_0 \geq 0, \ y\_0 \geq 0, v\_0 \geq 0, z\_0 \geq 0\}$.
Furthermore, we present the model's positivity, boundedness, and characteristic equilibria (disease-free and endemic equilibrium).

Lemma 1. *The solutions $((x(t), y(t), v(t), z(t)) \epsilon \ R_+^4)$ of the system (1)–(4) are positive at any time; $t \geq 0$ if the rate of change of state variables is non-negative at the trivial stage.*

Proof. The following is clear from Equations (1)–(4):
$\left.\frac{dx}{dt}\right|_{x=0} = r_1 \geq 0, \ \left.\frac{dy}{dt}\right|_{y=0} = axve_1^{-d_1\tau} \geq 0, \ \left.\frac{dv}{dt}\right|_{v=0} = by - h_2 yz \geq 0, \ \left.\frac{dz}{dt}\right|_{z=0} = m_1 v \geq 0$,
as required. $\square$

Lemma 2. *The solutions of (1)–(4) lie in the feasible region Ψ; $N(t)$ is the total population of cancer cells and $\lim_{t \to \infty} Sup \ N(t) \leq \frac{r_1}{d_1}$. Otherwise, the system is unbounded.*

Proof. Consider the cell population function as follows:

$$N(t) = x(t) + y(t) + v(t) + z(t), \ \frac{dN}{dt} \leq r_1 - d_1 N.$$

By using the Gronwall's inequality, we obtain the following:

$$N(t) \leq N(0)e^{-d_1 t} + \frac{r_1}{d_1}, \ t \geq 0, \lim_{t \to \infty} Sup \ N(t) \leq \frac{r_1}{d_1},$$

as required. $\square$

Lemma 3. *The system (1)–(4) admits two equilibria states, and both are contained in Ψ.*

Proof. Assume that the state variables of Equations (1)–(4) are constants.

Consider the $x \neq 0$, $y = 0$, $v = 0$, and $z = 0$ in the given system, and then we obtain the disease-free equilibrium (DFE-D_1) $= \left(\frac{r_1}{d_1}, 0, 0, 0\right)$. Then, by entering the $x \neq 0$, $y \neq 0$, $v \neq 0$, and $z \neq 0$ into the system and solving them simultaneously, the endemic equilibrium is obtained as follows: (EE-E_1) $= (x_1, y_1, v_1, z_1)$, where $x_1 = \frac{r_1}{av_1 + d_1}$, $y_1 = \frac{ar_1 v_1}{(av_1 + d_1)(cz_1 + d_1 + b)}$, $v^* = \frac{h_2 \beta z_1 - b\beta}{d_1 + m_1}$, $z_1 = \frac{m_1 \gamma}{c\beta + h_2 \beta - d_1}$. $\square$

2.2. Reproduction Number

To determine the reproduction number, let us apply the next-generation matrix method to find the transmission and transition matrices of the system (1)–(4) after substituting the disease-free equilibrium as follows:

$$
\begin{bmatrix} y' \\ v' \\ z' \end{bmatrix} = \begin{bmatrix} 0 & \frac{ar_1}{d_1} & 0 \\ 0 & 0 & 0 \\ 0 & 0 & 0 \end{bmatrix} \begin{bmatrix} y \\ v \\ z \end{bmatrix} - \begin{bmatrix} d_1 + b & 0 & 0 \\ -b & d_1 + m_1 & 0 \\ 0 & -m_1 & d_1 \end{bmatrix} \begin{bmatrix} y \\ v \\ z \end{bmatrix},
$$

$$
A = \begin{bmatrix} 0 & \frac{ar_1}{d_1} & 0 \\ 0 & 0 & 0 \\ 0 & 0 & 0 \end{bmatrix}, B = \begin{bmatrix} d_1 + b & 0 & 0 \\ -b & d_1 + m_1 & 0 \\ 0 & -m_1 & d_1 \end{bmatrix},
$$

$$
AB^{-1} = \begin{bmatrix} \frac{abr_1}{d_1(d_1+b)(d_1+m_1)} & \frac{ar_1}{d_1(d_1+m_1)} & 0 \\ 0 & 0 & 0 \\ 0 & 0 & 0 \end{bmatrix},
$$

$$
\left| AB^{-1} - \lambda \right| = \begin{vmatrix} \frac{abr_1}{d_1(d_1+b)(d_1+m_1)} - \lambda & \frac{ar_1}{d_1(d_1+m_1)} & 0 \\ 0 & 0 - \lambda & 0 \\ 0 & 0 & 0 - \lambda \end{vmatrix}.
$$

Hence, the dominant eigenvalue of the AB^{-1} is called the reproduction number and denoted as $R_0 = \frac{abr_1}{d_1(d_1+b)(d_1+m_1)}$.

2.3. Local Stability

In this section, we present two well-known theorems to determine the local stability of the model. Again, consider Equations (1)–(4) as a function of *F*, *G*, *H*, and *K* as follows:

$$
F = r_1 - axv - d_1x, \tag{5}
$$

$$
G = axv - cyz - d_1y - by, \tag{6}
$$

$$
H = by - h_2yz - d_1v - m_1v, \tag{7}
$$

$$
K = cyz + h_2yz - d_1z + m_1v. \tag{8}
$$

The Jacobian matrix for the system (5)–(8) becomes the following:

$$
J(x, y, v, z) = \begin{bmatrix} -av - d_1 & 0 & -ax & 0 \\ av & -cz - d_1 - b & ax & -cy \\ 0 & b - h_2z & -d_1 - m_1 & -h_2y \\ 0 & cz + h_2z & m_1 & cy + h_2y - d_1 \end{bmatrix} \tag{9}
$$

Theorem 1. *If the reproduction number $R_0 < 1$, then the disease-free equilibrium (DFE),* $D_1 = \left(\frac{r_1}{d_1}, 0, 0, 0 \right)$, *is locally and asymptotically stable. Otherwise, the system is unstable.*

Proof. The Jacobian matrix (9) at the disease-free equilibrium, $D_1 = \left(\frac{r_1}{d_1}, 0, 0, 0 \right)$, is evaluated as follows:

$$
J\left(\frac{r_1}{d_1}, 0, 0, 0 \right) = \begin{bmatrix} -d_1 & 0 & -a\left(\frac{r_1}{d_1}\right) & 0 \\ 0 & -d_1 - b & a\left(\frac{r_1}{d_1}\right) & 0 \\ 0 & b & -d_1 - m_1 & 0 \\ 0 & 0 & m_1 & -d_1 \end{bmatrix},
$$

$$|J(D_1) - \lambda I| = \begin{vmatrix} -d_1 - \lambda & 0 & -a\left(\frac{r_1}{d_1}\right) & 0 \\ 0 & -d_1 - b - \lambda & a\left(\frac{r_1}{d_1}\right) & 0 \\ 0 & b & -d_1 - m_1 - \lambda & 0 \\ 0 & 0 & m_1 & -d_1 - \lambda \end{vmatrix} = 0,$$

$$\lambda_1 = -d_1 < 0, \lambda_2 = -d_1 < 0,$$

$$|J(D_1) - \lambda I| = \begin{vmatrix} -d_1 - b - \lambda & \frac{ar_1}{d_1} \\ b & -d_1 - m_1 - \lambda \end{vmatrix} = 0,$$

$$\lambda^2 + A_1\lambda + A_2 = 0,$$

where $A_1 = 2d_1 + b$ and $A_2 = d_1^2 + m_1 d_1 + bm_1 + bd_1 + \frac{abr_1}{d_1}$, if $R_0 < 1$. $\square$

All coefficients of the polynomial are positive. Therefore, the Routh–Hurwitz stability criterion for a 2nd-degree polynomial is satisfied. Therefore, the disease-free equilibrium is stable.

Theorem 2. *If $R_0 > 1$, then the endemic equilibrium (EE), $E_1 = (x_1, y_1, v_1, z_1)$, is locally and asymptotically stable.*

Proof. The Jacobian matrix (9) at the endemic equilibrium, $E_1 = (x_1, y_1, v_1, z_1)$, is as follows:

$$J(x_1, y_1, v_1, z_1,) = \begin{bmatrix} av_1 - d_1 & 0 & ax_1 & 0 \\ av_1 & -cz_1 - d_1 - b & ax_1 & -cy_1 \\ 0 & b - h_2 z_1 & -d_1 - m_1 & -h_2 y_1 \\ 0 & cz_1 + h_2 z_1 & m_1 & cy_1 + h_2 y_1 - d_1 \end{bmatrix},$$

$$|J(E_1) - \lambda I| = \begin{vmatrix} av_1 - d_1 & 0 & ax_1 & 0 \\ av_1 & -cz_1 - d_1 - b & ax_1 & -cy_1 \\ 0 & b - h_2 z_1 & -d_1 - m_1 & -h_2 y_1 \\ 0 & cz_1 + h_2 z_1 & m_1 & cy_1 + h_2 y_1 - d_1 \end{vmatrix} = 0,$$

$$\lambda^4 + (A + d_1 + F - I - B)\lambda^3 + (AF - AB - AI - d_1 F - DF + BI - FI - CF - DH)\lambda^2 - (ABI - ABF - AFI - ACE - ADH + d_1 BI - d_1 BF - d_1 FI - d_1 I - d_1 CE - d_1 DH + BFI + m_1 G + CEI - CGH - CEm_1 - DHF + ACE)\lambda + (ABFI + AGm_1 + ACEI - ACGH - ADEm_1 - ADHF + BFTd_1 + Gd_1 m_1 + d_1 CEI - CGHd_1 - DEm_1 d_1 - DHFd_1 - ACEI + ACHG) = 0,$$

where $A = av_1, B = -d_1 - b - cy_1, C = ax_1, D = -cy_1, E = b - h_2 z_1, F = d_1 + m_1$

$$G = -h_2 y_1, \quad H = cz + h_2 z_1, \text{ and } I = cy_1 - d_1 + h_2 y_1.$$

By considering the coefficients of the characteristic equation above as a 4th-order polynomial, we have the following:

$$m_0, m_1 > 0, \ m_1 m_2 - m_0 m_3 > 0, \ (m_1 m_2 - m_0 m_3)(m_3) - m_1{}^2 m_4 > 0, \ m_4 > 0, \text{ if } R_O > 1.$$

where $m_0 = 1$, $m_1 = A + d_1 + F - I - B$, $m_2 = AF - AB - AI - d_1 F - DF + BI - FI - CF - DH$, $m_3 = ABI - ABF - AFI - ACE - ADH + d_1 BI - d_1 BF - d_1 FI - d_1 I - d_1 CE - d_1 DH + BFI + m_1 G + CEI - CGH - CEm_1 - DHF + ACE$, $m_4 = ABFI + AGm_1 + ACEI - ACGH - ADEm_1 - ADHF + BFTd_1 + Gd_1 m_1 + d_1 CEI - CGHd_1 - DEm_1 d_1 - DHFd_1 - ACEI + ACHG$. $\square$

It satisfies the Routh–Hurwitz stability criterion for a 4th-degree polynomial. Therefore, the endemic equilibrium is also stable.

3. Stochastic Cancer Virotherapy Model

Let us consider the vector $M = [x, y, v, z]^T$ for the system (1)–(4). Transition probabilities are presented in Table 1 for the expectations and variance.

Table 1. Transition probabilities of cancer epidemic model.

T_i=Transition	P_i=Probabilities
$T_1 = [1, 0, 0, 0]^T$	$P_1 = r_1 \Delta t$
$T_2 = [-1, 1, 0, 0]^T$	$P_2 = axv.\Delta t$
$T_3 = [-1, 0, 0, 0]^T$	$P_3 = d_1 x \Delta t$
$T_4 = [0, -1, 0, 1]^T$	$P_4 = cyz \Delta t$
$T_5 = [0, -1, 0, 0]^T$	$P_5 = d_1 y \Delta t$
$T_6 = [0, -1, 1, 0]^T$	$P_6 = by \Delta t$
$T_7 = [0, 0, -1, 1]^T$	$P_7 = h_2 yz \Delta t$
$T_8 = [0, 0, -1, 0]^T$	$P_8 = d_1 v \Delta t$
$T_9 = [0, 0, -1, 1]^T$	$P_9 = m_1 v \Delta t$
$T_{10} = [0, 0, 0, -1]^T$	$P_{10} = d_1 z \Delta t$

Expectation $= E^*[\Delta M_i] = \sum_{i=1}^{10} P_i T_i$

$$= \begin{bmatrix} P_1 - P_2 - P_3 \\ P_2 - P_4 - P_5 - P_6 \\ P_6 + P_7 - P_8 - P_9 \\ P_4 - P_7 - P_9 - P_{10} \end{bmatrix} = \begin{bmatrix} r_1 - axv - d_1 x \\ axv - cyz - d_1 y - by \\ by + h_2 yz - d_1 v - m_1 v \\ cyz - h_2 yz - m_1 v - d_1 z \end{bmatrix} \Delta t,$$

Variance $= \sum_{i=1}^{10} (T_i)(T_i)^t$

$$= \begin{bmatrix} P_1 + P_2 + P_3 & P_2 & 0 & 0 \\ -P_2 & P_2 + P_4 + P_5 + P_6 & -P_6 & -P_4 \\ 0 & -P_6 & P_6 + P_7 + P_8 + P_9 & -P_7 + P_9 \\ 0 & -P_4 & -P_7 + P_9 & P_4 + P_7 + P_9 + P_{10} \end{bmatrix}$$

$$= \begin{bmatrix} a_{11} & a_{12} & a_{13} & a_{14} \\ a_{21} & a_{22} & a_{23} & a_{24} \\ a_{31} & a_{32} & a_{33} & a_{34} \\ a_{41} & a_{42} & a_{43} & a_{44} \end{bmatrix}$$

$a_{11} = P_1 + P_2 + P_3 = r_1 - axv - d_1 x$, $a_{13} = a_{14} = a_{31} = a_{41} = 0$, $a_{12} = P_2 = axv$, $a_{21} = -P_2 = -avx$, $a_{22} = P_2 + P_4 + P_5 + P_6 = axv + cyz + d_1 y + by$, $a_{23} = -P_6 = -by$, $a_{24} = -P_4 = -cyz$, $a_{32} = -P_6 = -by$, $a_{33} = P_6 + P_7 + P_8 + P_9 = by + h_2 yz + d_1 v + m_1 v$, $a_{42} = -P_4 = -cyz$, $a_{43} = -P_7 + P_9 = -h_2 yz + m_1 v$, $a_{44} = P_4 + P_7 + P_9 + P_{10} = cyz + h_2 yz + m_1 v + d_1 z$,

$$\text{Drift} = G_1(M, t) = \frac{expectation}{\Delta t} = \begin{bmatrix} r_1 - axv - d_1 x \\ axv - cyz - d_1 y - by \\ by + h_2 yz - d_1 v - m_1 v \\ cyz - h_2 yz - m_1 v - d_1 z \end{bmatrix} \Delta t,$$

$$\text{Diffusion} = G_2(M, t) = \sqrt{\frac{Variance}{\Delta t}} = \sqrt{A}, \text{where } A = \begin{bmatrix} a_{11} & a_{12} & a_{13} & a_{14} \\ a_{21} & a_{22} & a_{23} & a_{24} \\ a_{31} & a_{32} & a_{33} & a_{34} \\ a_{41} & a_{42} & a_{43} & a_{44} \end{bmatrix}.$$

The stochastic differential equations (SDEs) of the cancer virotherapy model for the system (1)–(4) are presented as follows:

$$dM = G_1(M, t)dt + G_2(M, t)dB,$$ (10)

$$d\begin{bmatrix} x \\ y \\ v \\ z \end{bmatrix} = \begin{bmatrix} r_1 - axv - d_1x \\ axv - cyz - d_1y - by \\ by + h_2yz - d_1v - m_1v \\ cyz - h_2yz - m_1v - d_1z \end{bmatrix} dt + \sqrt{A}\,dB$$ (11)

with initial conditions $M(0) = M_0 = [0.5, 0.3, 0.2, 0.1]^T$, $0 \le t \le M$, and B is Brownian motion.

3.1. Euler Maruyama Method

In this section, we utilize the Euler Maruyama scheme to determine the numerical solution of differential Equation (11), and the scientific parameters of the model are presented in Table 2 as follows:

$$M_{n+1} = M_n + G_1(M_n, t)\Delta t + G_2(M_n, t)\Delta B_n,$$

$$\begin{bmatrix} x^{n+1} \\ y^{n+1} \\ v^{n+1} \\ z^{n+1} \end{bmatrix} = \begin{bmatrix} x^n \\ y^n \\ v^n \\ z^n \end{bmatrix} + \begin{bmatrix} r_1 - axv - d_1x \\ axv - cyz - d_1y - by \\ by + h_2yz - d_1v - m_1v \\ cyz - h_2yz - m_1v - d_1z \end{bmatrix} \Delta t + \sqrt{A}\,\Delta B_n,$$ (12)

where Δt is the time-step size, and ΔB_n is the discretization parameter independent paths. By using the values of the parameters presented in Table 2, we plotted the graphs of the Euler Maruyama scheme for disease-free equilibrium (DFE) and endemic equilibrium (EE) (see Figures 2 and 3) with MATLAB software.

Table 2. Parameter estimation (fitted data).

Parameters	Values
r_1	0.5
a	5.1 (EE) 3.1 (DFE)
h_1	0.63
d_1	0.5
C	5.048 (EE) 3.048 (DFE)
b	0.22
h_2	0.016
m_1	0.6
σ_i	$0 \le i \le 1$

3.2. Data Curation

In 2020, the total population of both sexes was approximately 220,892,332, which includes the male sex (113,672,007) and the female sex (107,220,324) [20]. The number of new cases of both sexes and all ages is shown in Figure 4. Using the least-square-curve method technique, the desired fitting is presented in Figure 5. The estimated values from the data are presented in Table 2, and the value of the reproduction number is $R_0 = 1.4167$. Furthermore, Figure 6 depicts the residual of the actual data. Hence, the desired values of the transmission rates are helpful to study the system (1)–(4) graphically.
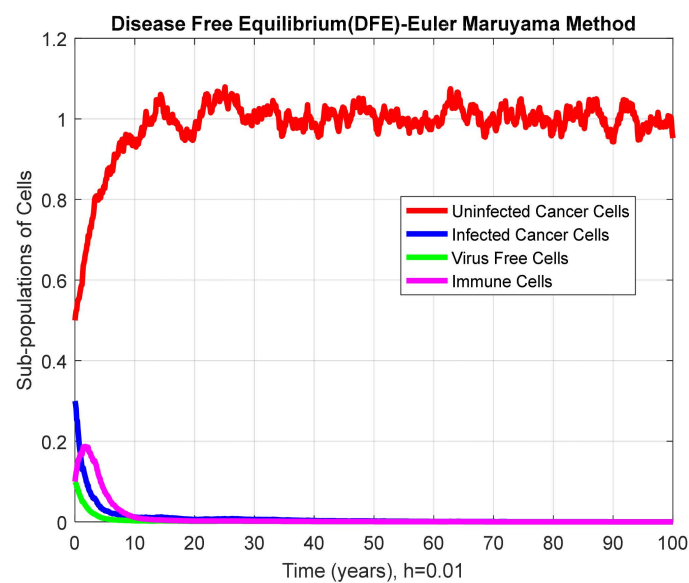
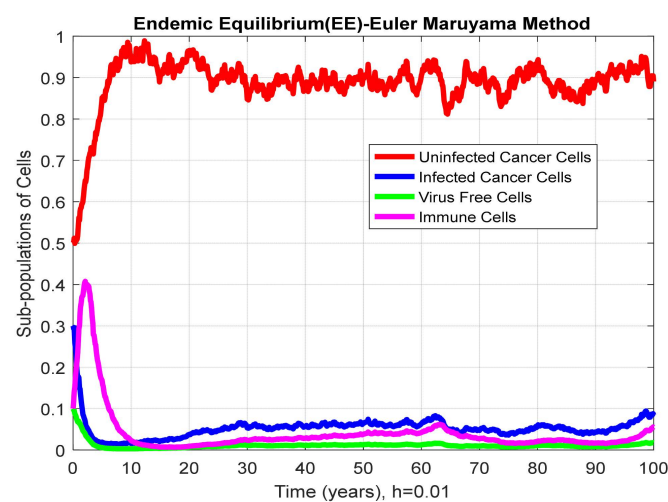**Figure 2.** Combined graphical behavior of subpopulations at DFE for h = 0.01.

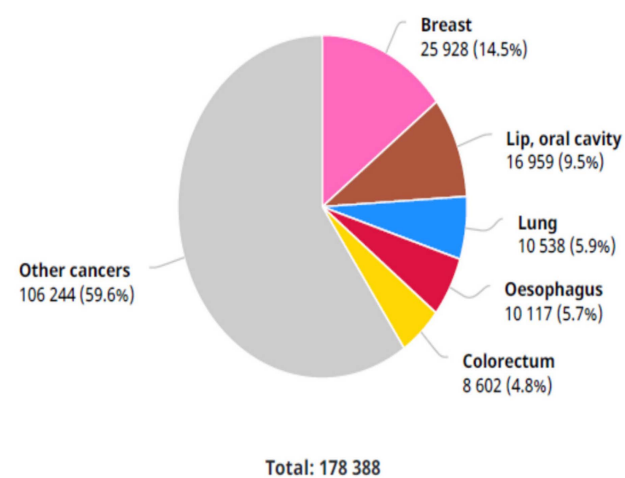**Figure 3.** Combined graphical behavior of subpopulations at EE for h = 0.01.
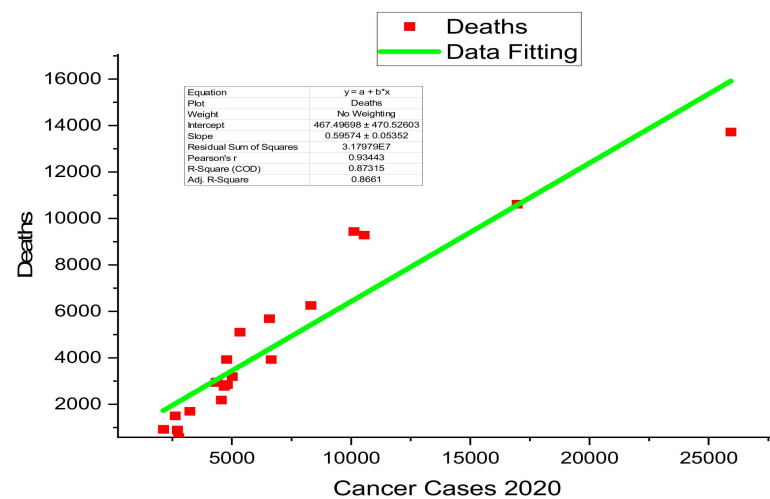

Figure 4. Ratio of cancer cases.

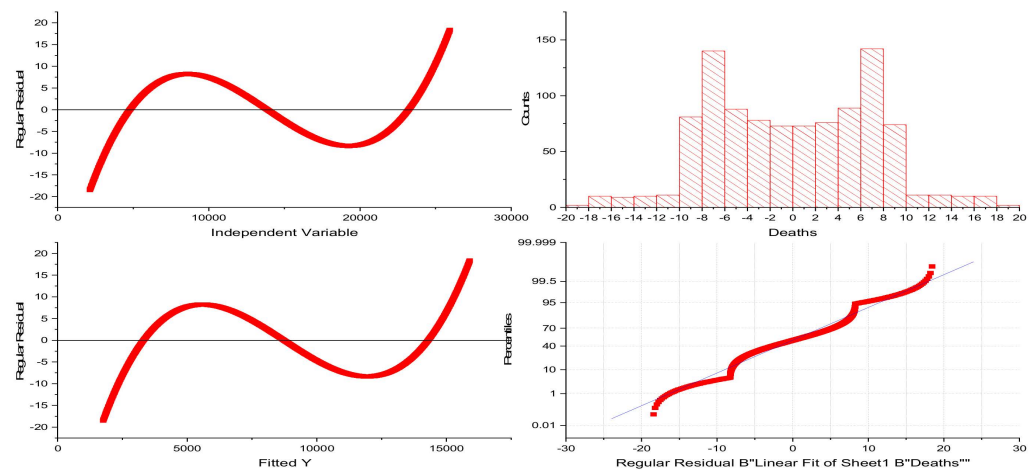**Figure 5.** Least-square data-fitting presentation of cancer cases.

Figure 6. Regular-residuals of cancer cases in 2020.

3.3. Non-Parametric Perturbation of Model

This section introduces the stochasticity in each compartment of the system (1)–(4). Then Equations (1)–(4) become as follows:

$$dx(t) = r_1 - ax(t)v(t) - d_1 x(t) + \sigma_1 x dB(t), \ t \geq 0, \tag{13}$$

$$dy(t) = ax(t)v(t) - cy(t)z(t) - d_1 y(t) - by(t) + \sigma_2 y(t)dB(t), \ t \geq 0, \tag{14}$$

$$dv(t) = by(t) - h_2 y(t)z(t) - d_1 v(t) - m_1 v(t) + \sigma_3 v(t)dB(t), \ t \geq 0, \tag{15}$$

$$dz(t) = cy(t)z(t) + h_2 y(t)z(t) - d_1 z(t) + m_1 v(t) + \sigma_4 z(t)dB(t), \ t \geq 0, \tag{16}$$

where, for σ_i, $i = 1, 2, 3, 4$ is the randomness of the model; and B(t) is the Brownian motion.

3.4. Positivity and Boundedness of Stochastic Model

Consider $U(t) = (x(t), y(t), v(t), z(t))$, and the norm:

$$|U(t)| = \sqrt{x^2(t) + y^2(t) + v^2(t) + z^2(t)} \tag{17}$$

In addition, denote $C_1^{2,1}(R^4 \times (0, \infty) : R_+)$ as the families of all positive function $V(U, t)$ defined on $R^4 \times (0, \infty)$ respectively. Let the function be twice differentiable in U and once in t, and then we have the following:

$$dU(t) = H_1(U, t) + K_1(U, t)dB(t) \tag{18}$$

Additionally, $L = \frac{\partial}{\partial t} + \sum_{i=1}^{3} H_{1_i}(U, t)\frac{\partial}{\partial U_i} + \frac{1}{2} \sum_{i,j=1}^{3} (K_1^T(U, t)K_1(U, t)_{i,j} \times \frac{\partial^2}{\partial U_i \partial U_j})$.

If "L" acts on a function $U^* \epsilon C^{2,1}(R^4 \times (0, \infty) : R_+^4)$, then

$$LU^*(U, t) = U_t^*(U, t) + U_U^*(U, t)H_1(U, t) + \frac{1}{2}Trace\left(K_1^T(U, t)U_{UU}^*(U, t)K_1(U, t)\right),$$

where t means transpose.

Theorem 3. *A unique solution* $(x(t), y(t), v(t), z(t))$, $t \geq 0$ *of the system (13)–(16) lies in* R_+^4 *with initial conditions* $(x(0), y(0), v(0), z(0)) \epsilon R_+^4$.

Proof. By Ito's formula, (13)–(16) admit positive solution in the sense of local on $[0, \tau_e]$, while τ_e denotes the explosion time, due to the local Lipschitz coefficients of the model.

Next, we prove that the system (13)–(16) model admits $\tau_e = \infty$.

Let $m_0 = 0$ be sufficiently large for $x(0)$, $y(0)$, $v(0)$, and $z(0)$ lying in the interval $\left(\frac{1}{m_0}, m_0\right)$.

A sequence at stopping times $m \geq 0$ is defined as follows:

$$\tau_m = \inf\left\{\tau \epsilon [0, \tau_e] : x(t)\left(\frac{1}{m}, m\right) or \ y(t)\left(\frac{1}{m}, m\right) or \ z(t)\left(\frac{1}{m}, m\right) or \ w(t)\left(\frac{1}{m}, m\right)\right\}, \tag{19}$$

where we set $\inf \varphi = \infty(\varphi$ is an empty set).

Since τ_m is increasing as $m \to \infty$, we have the following:

$$\tau_\infty = \lim_{m \to \infty} \tau_m. \tag{20}$$

Then $\tau_\infty \leq \tau_e$. Now we wish to show that $\tau_\infty = \infty$, as desired.

$$P(\tau_\infty \leq T) > a_1, \ \forall m \geq m_1, \tag{21}$$

$$P(\tau_m \leq T) > a_1, \ \forall m \geq m_1. \tag{22}$$

Define a function $f : R_+^4 \to R_+$ by using the following calculation:

$$f(x, y, v, z) = (x - 1 - \ln x) + (y - 1 - \ln y) + (v - 1 - \ln v) + (z - 1 - \ln z). \tag{23}$$

Using Ito's formula on (23), we have the following:

$$df(x, y, v, z) = \left(1 - \frac{1}{x}\right)dx + \left(1 - \frac{1}{y}\right)dy + \left(1 - \frac{1}{v}\right)dv + \left(1 - \frac{1}{z}\right)dz + \frac{\sigma_1^2 + \sigma_2^2 + \sigma_3^2 + \sigma_4^2}{2}dt,$$

$$df(x, y, v, z) = \left(1 - \frac{1}{x}\right)[r_1 - axv - d_1x + \sigma_1 xdB] + \left(1 - \frac{1}{y}\right)[axv - cyz - d_1y - by + \sigma_2 ydB]$$

$$+ \left(1 - \frac{1}{v}\right)[by - h_2yz - d_1v - m_1v + \sigma_3 vdB] + \left(1 - \frac{1}{z}\right)[cyz + h_2yz - d_1z + m_1v + \sigma_4 zdB], \tag{24}$$

$$df(x, y, v, z) \leq \left[r_1 + d_1 + \frac{\sigma_1^2 + \sigma_2^2 + \sigma_3^2 + \sigma_4^2}{2}\right]dt + \sigma_1 xdB + \sigma_2 ydB + \sigma_3 vdB + \sigma_4 zdB.$$

For simplicity, we let $N_1 = r_1 + d_1 + \frac{\sigma_1^2 + \sigma_2^2 + \sigma_3^2 + \sigma_4^2}{2}$ and write Equation (24) as follows:

$$df(x, y, v, z) \leq N_1 dt + [\sigma_1 x + \sigma_2 y + \sigma_3 v + \sigma_4 z]dB(t). \tag{25}$$

The N_1 is a positive constant. By integrating Equation (25) from 0 to $\tau_m \Lambda \tau$, we obtain the following:

$$\int_0^{\tau_m \Lambda \tau} df(x, y, z, w) \leq \int_0^{\tau_m \Lambda \tau} N_1 ds + \int_0^{\tau_m \Lambda \tau} [\sigma_1 x + \sigma_2 y + \sigma_3 v + \sigma_4 z] dB(s), \quad (26)$$

where $\tau_m \Lambda \tau = \min(\tau_m, T)$. Then the expectation is as follows:

$$EU^*(x(\tau_m \Lambda \tau), y(\tau_m \Lambda \tau), v(\tau_m \Lambda \tau), z(\tau_m \Lambda \tau) \leq U^*(x(0), y(0), v(0), z(0)) + N_1 T. \quad (27)$$

Set $\chi_m = \{\tau_m \leq T\}$ for $m > m_1$ and from Equation (20), and we have $P(\chi_m \geq a_1)$.

For every $\chi_1 \epsilon \chi_m$, there are some "I's" such that $U_i(\tau_m, \chi_1)$ equals either m or $\frac{1}{m}$ for i = 1, 2, 3, 4. Hence, we have the following:

$$U^*(x(\tau_m, \chi_1), y(\tau_m, \chi_1), z(\tau_m, \chi_1), w(\tau_m, \chi_1)).$$

For "I" less than $\min\left(m - 1 - \ln m, \frac{1}{m} - 1 - \ln \frac{1}{m}\right\}$, we then obtain the following:

$$U^*(x(0), y(0), v(0), z(0)) + N_1 T \geq E(I_{\chi_\chi} U^*(x(\tau_m), y(\tau_m), v(\tau_m), z(\tau_m)) \geq$$
$$\left\{ min\{m - 1 - \ln m, \tfrac{1}{m} - 1 - \ln \tfrac{1}{m}\}\right\}. \quad (28)$$

Iχ of χm represents the indicator functions. Letting $m \to \infty$ leads to the contradiction $\infty = U^*(x(0), y(0), v(0), z(0)) + N_1 T < \infty$, as desired. $\quad \square$

4. Computational Methods

This section deals with well-known methods, such as the stochastic Euler, the stochastic Runge Kutta, and the proposed stochastic nonstandard finite difference method with the given non-negative initial conditions as follows:

4.1. Stochastic Euler

The stochastic Euler method could be defined on the system (13)–(16). (See Appendix A).

4.2. Stochastic Runge Kutta

The stochastic Runge Kutta method could be developed on the system (13)–(16). (See Appendix B).

4.3. Stochastic NSFD

The stochastic nonstandard finite difference could be developed for the system (13)–(16). (See Appendix C).

4.4. Stability Analysis

This section determines the model's stability by considering the equilibrium state and the theorem. The model is linearized for the stochastic nonstandard finite difference. (See Appendix D).

Lemma 4. *For the quadratic equation $\lambda^2 - P_1 \lambda + P_2 = 0$, $|\lambda_i| < 1$, $i = 1, 2, 3$, if and only if the following conditions are satisfied:*
(i) $1 + P_1 + P_2 > 0.$
(ii) $1 - P_1 + P_2 > 0.$
(iii) $P_2 < 1.$

Proof. The proof is straightforward. $\quad \square$

4.5. Comparison Section

The stochastic nonstandard finite difference method was compared with other stochastic numerical methods. It is easy to see that other stochastic numerical methods conditionally converge or diverge with larger time-step values by looking at the numerical solutions. On the other hand, the stochastic nonstandard finite-difference scheme remains convergent for all time-step sizes. Figures 7–12 show these results.
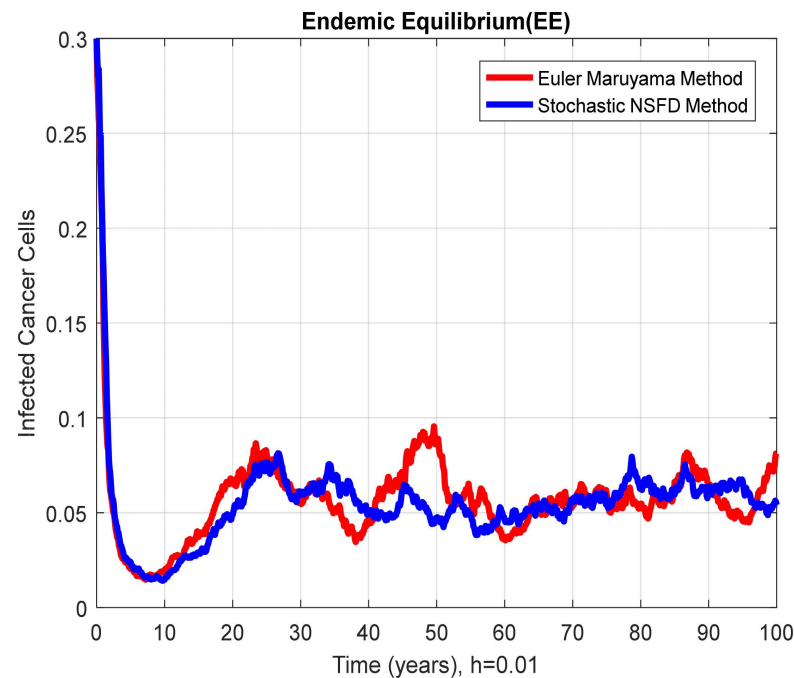

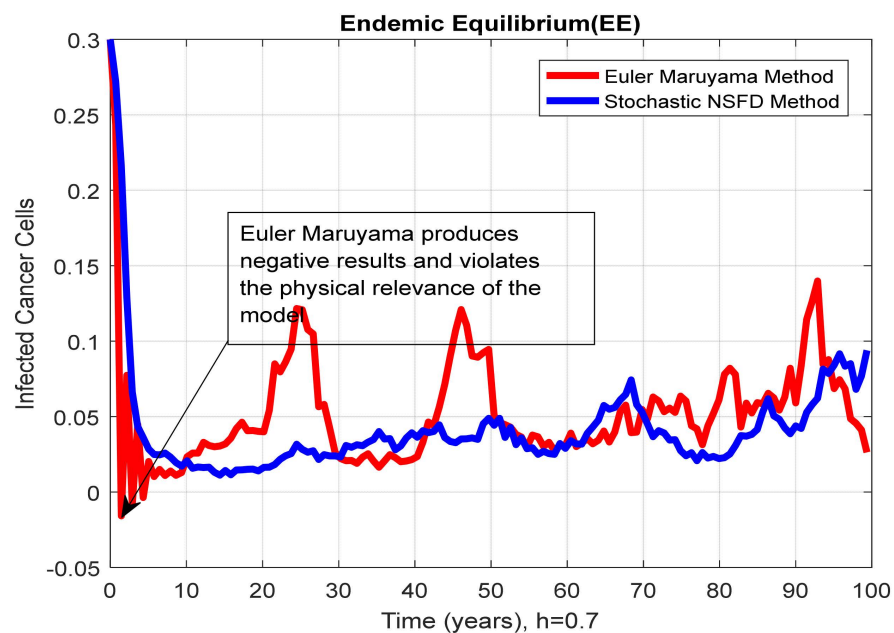**Figure 7.** Combined behavior of infected cancer cells at EE when h = 0.01.

Figure 8. Combined behavior of infected cancer cells at EE when h = 0.7. Here, notice that, when we increase a time-step size, the Euler Maruyama method fails to restore the dynamical properties of the model.
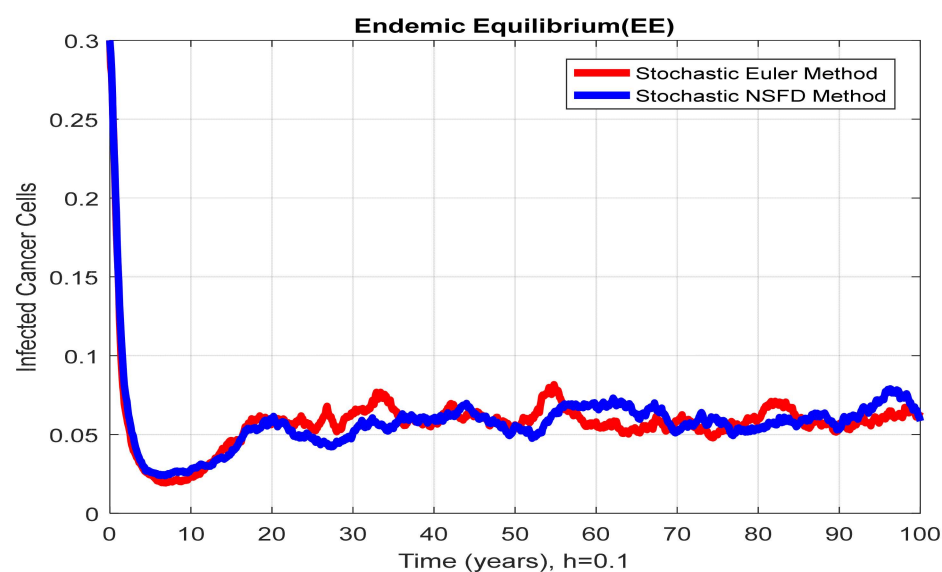
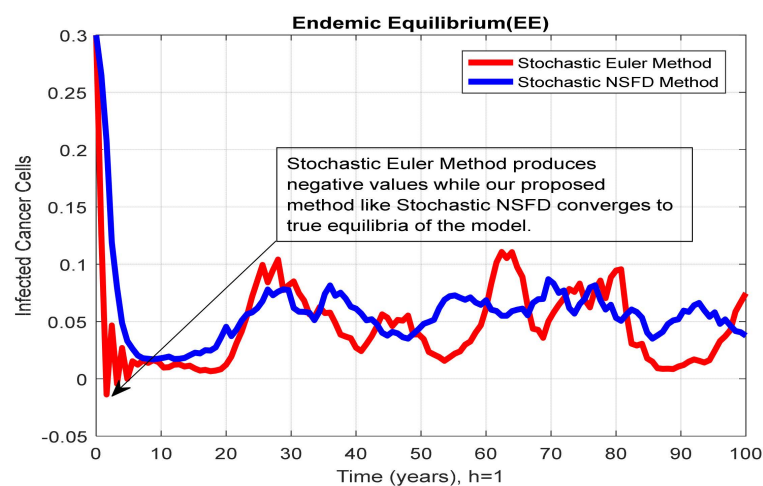**Figure 9.** Combined behavior of infected cancer cells at EE when h = 0.1.

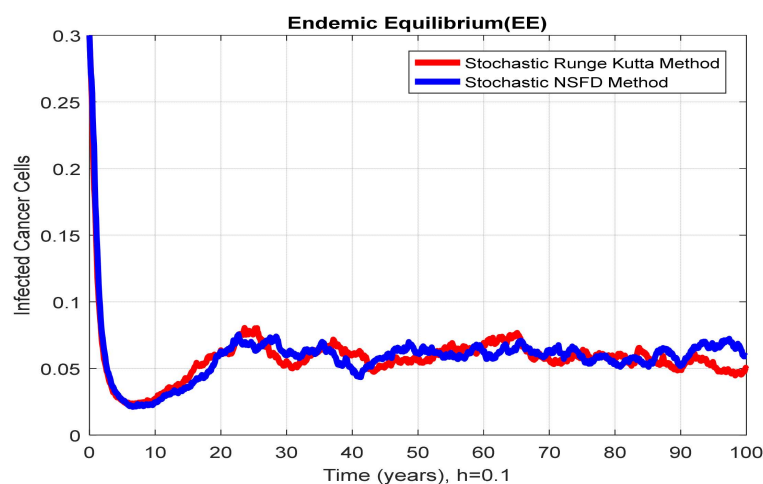**Figure 10.** Combined behavior of infected cancer cells at EE when h = 1.

Figure 11. Combined behavior of infected cancer cells at EE when h = 0.1.
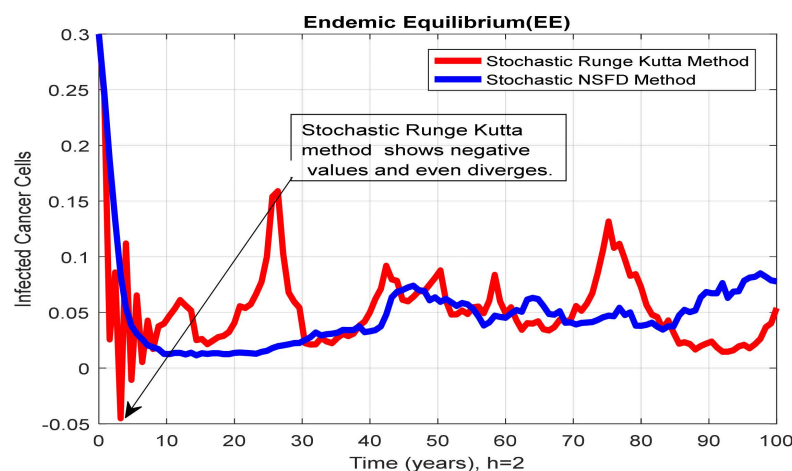
Figure 12. Combined behavior of infected cancer cells at EE when h = 2. Here, notice that, when we increase a time-step size, the Stochastic Runge-Kutta method fails to restore the dynamical properties of the model. However, the stochastic nonstandard finite difference method is still convergent.

5. Conclusions

Stochastic modeling is a reliable and efficient technique for handling highly nonlinear problems' natural phenomena. The non-parametric perturbation technique was used in establishing the stochastic cancer virotherapy model. The nonstandard finite difference method gives dynamically consistent, positive, and bounded solutions. It is believed that existing algorithms did not restore the dynamical properties of the model, such as positivity, boundedness, and dynamical consistency, when we take a considerable time-step size. However, the nonstandard finite-difference scheme solved the problem competitively and out-performed the standard methods that were compared in this work. This is visibly noticed in the unconditional convergence of the solution given by the nonstandard finite-difference scheme against the conditional convergence or divergence offered by the existing methods. It further shows that the approach by the nonstandard finite difference is novel and can be applied to solving other nonlinear stochastic problems. The following steps are helpful to reduce the risk of getting cancer by making healthy choices, such as maintaining a healthy weight, avoiding tobacco, limiting the amount of alcohol, and protecting the skin. In the future, we will extend the idea used in this work to different types of stochastic modeling; moreover, its stabilities are presented in References [26–34].

Author Contributions: Conceptualization, investigation, and original draft, A.R.; supporting and visualization, J.A.; methodology and lead M.R.; supervision and investigation, N.A.; visualization, formal analysis, and writing—review and editing, M.M. All authors have read and agreed to the published version of the manuscript.

Appendix A

$$dx = (r_1 - axv - d_1x)dt + \sigma_1 x dB(t),$$
$$\frac{x^{n+1} - x^n}{h} = r_1 - ax^n v^n - d_1 x^n + \sigma_1 x^n \Delta B_n,$$
$$x^{n+1} = x^n + h[r_1 - ax^n v^n - d_1 x^n + \sigma_1 x^n \Delta B_n].$$

(A1)

Similarly, the decomposition of these equations is shown in (A2)–(A4)

$$y^{n+1} = y^n + h[ax^n v^n - cy^n z^n - d_1 y^n - by^n + \sigma_2 y^n \Delta B_n], \tag{A2}$$

$$v^{n+1} = v^n + h[by^n - h_2 y^n z^n - d_1 v^n - m_1 v^n + \sigma_3 v^n \Delta B_n], \tag{A3}$$

$$z^{n+1} = z^n + h[cy^n z^n + h_2 y^n z^n - d_1 z^n + m_1 v^n + \sigma_4 z^n \Delta B_n], \tag{A4}$$

Appendix B

Stage 1

$$K_1 = h[r_1 - ax^n v^n - d_1 x^n + \sigma_1 x^n \Delta B_n],$$
$$L_1 = h[ax^n v^n - cy^n z^n - d_1 y^n - by^n + \sigma_2 y^n \Delta B_n],$$
$$M_1 = h[by^n - h_2 y^n z^n - d_1 v^n - m_1 v^n + \sigma_3 v^n \Delta B_n],$$
$$N_1 = h[cy^n z^n + h_2 y^n z^n - d_1 z^n + m_1 v^n + \sigma_4 z^n \Delta B_n].$$

Stage 2

$$K_2 = h\left[r_1 - a\left(x^n + \frac{K_1}{2}\right)\left(v^n + \frac{K_1}{2}\right) - d_1\left(x^n + \frac{K_1}{2}\right) + \sigma_1\left(x^n + \frac{K_1}{2}\right)\Delta B_n\right],$$
$$L_2 = h\left[a\left(x^n + \frac{L_1}{2}\right)\left(v^n + \frac{L_1}{2}\right) - c\left(y^n + \frac{L_1}{2}\right)\left(z^n + \frac{L_1}{2}\right) - d_1\left(y^n + \frac{L_1}{2}\right) - b\left(y^n + \frac{L_1}{2}\right) + \sigma_2\left(y^n + \frac{L_1}{2}\right)\Delta B_n\right],$$
$$M_2 = h\left[b\left(y^n + \frac{M_1}{2}\right) - h_2\left(y^n + \frac{M_1}{2}\right)\left(z^n + \frac{M_1}{2}\right) - d_1\left(v^n + \frac{M_1}{2}\right) - m_1\left(v^n + \frac{M_1}{2}\right) + \sigma_3\left(v^n + \frac{M_1}{2}\right)\Delta B_n\right],$$
$$N_2 = h\left[c\left(y^n + \frac{N_1}{2}\right)\left(z^n + \frac{N_1}{2}\right) + h_2\left(y^n + \frac{N_1}{2}\right)\left(z^n + \frac{N_1}{2}\right) - d_1\left(z^n + \frac{N_1}{2}\right) + m_1\left(v^n + \frac{N_1}{2}\right) + \sigma_4\left(z^n + \frac{N_1}{2}\right)\Delta B_n\right].$$

Stage 3

$$K_3 = h\left[r_1 - a\left(x^n + \frac{K_2}{2}\right)\left(v^n + \frac{K_2}{2}\right) - d_1\left(x^n + \frac{K_2}{2}\right) + \sigma_1\left(x^n + \frac{K_2}{2}\right)\Delta B_n\right],$$
$$L_3 = h\left[a\left(x^n + \frac{L_2}{2}\right)\left(v^n + \frac{L_2}{2}\right) - c\left(y^n + \frac{L_2}{2}\right)\left(z^n + \frac{L_2}{2}\right) - d_1\left(y^n + \frac{L_2}{2}\right) - b\left(y^n + \frac{L_2}{2}\right) + \sigma_2\left(y^n + \frac{L_2}{2}\right)\Delta B_n\right],$$
$$M_3 = h\left[b\left(y^n + \frac{M_2}{2}\right) - h_2\left(y^n + \frac{M_2}{2}\right)\left(z^n + \frac{M_2}{2}\right) - d_1\left(v^n + \frac{M_2}{2}\right) - m_1\left(v^n + \frac{M_2}{2}\right) + \sigma_3\left(v^n + \frac{M_2}{2}\right)\Delta B_n\right],$$
$$N_3 = h\left[c\left(y^n + \frac{N_2}{2}\right)\left(z^n + \frac{N_2}{2}\right) + h_2\left(y^n + \frac{N_2}{2}\right)\left(z^n + \frac{N_2}{2}\right) - d_1\left(z^n + \frac{N_2}{2}\right) + m_1\left(v^n + \frac{N_2}{2}\right) + \sigma_4\left(z^n + \frac{N_2}{2}\right)\Delta B_n\right].$$

Stage 4

$$K_4 = h[r_1 - a(x^n + K_3)(v^n + K_3) - d_1(x^n + K_3) + \sigma_1(x^n + K_3)\Delta B_n],$$
$$L_4 = h[a(x^n + L_3)(v^n + L_3) - c(y^n + L_3)(z^n + L_3) - d_1(y^n + L_3) - b(y^n + L_3) + \sigma_2(y^n + L_3)\Delta B_n],$$
$$M_4 = h[b(y^n + M_3) - h_2(y^n + M_3)(z^n + M_3) - d_1(v^n + M_3) - m_1(v^n + M_3) + \sigma_3(v^n + M_3)\Delta B_n],$$
$$N_4 = h[c(y^n + N_3)(z^n + N_3) + h_2(y^n + N_3)(z^n + N_3) - d_1(z^n + N_3) + m_1(v^n + N_3) + \sigma_4(z^n + N_3)\Delta B_n].$$

Final Stage

$$x^{n+1} = x^n + \frac{1}{6}[K_1 + 2K_2 + 2K_3 + K_4], \tag{A5}$$

$$y^{n+1} = y^n + \frac{1}{6}[L_1 + 2L_2 + 2L_3 + L_4], \tag{A6}$$

$$v^{n+1} = v^n + \frac{1}{6}[M_1 + 2M_2 + 2M_3 + M_4], \tag{A7}$$

$$z^{n+1} = z^n + \frac{1}{6}[N_1 + 2N_2 + 2N_3 + N_4], \tag{A8}$$

Appendix C

$$x^{n+1} = x^n + h\left[r_1 - ax^{n+1}v^n - d_1x^{n+1} + \sigma_1 x^n \Delta B_n\right],$$

$$x^{n+1} = \frac{x^n + h\gamma + h\sigma_1 x^n \Delta B_n}{1 + ahv^n + hd_1}. \tag{A9}$$

In the same way, we decompose the remaining system as follows:

$$y^{n+1} = \frac{y^n + hax^n v^n + h\sigma_2 y^n \Delta B_n}{1 + hcz^n + hd_1 + hb} \tag{A10}$$

$$v^{n+1} = \frac{v^n + hby^n - hh_2 y^n z^n + h\sigma_3 v^n \Delta B_n}{1 + hd_1 + hm_1} \tag{A11}$$

$$z^{n+1} = \frac{z^n + hcy^n z^n + hh_2 y^n z^n + hm_1 v^n + h\sigma_4 z^n \Delta B_n}{1 + hd_1} \tag{A12}$$

Appendix D

Theorem A1. *For any $n \geq 0$, the proposed nonstandard finite difference method is stable if the eigenvalues of the system (A9)–(A12) lie in the unit circle for $R_0 < 1$.*

Proof. Consider the right-hand sides of the system of Equations (A9)–(A12) as functions F, G, H, and J, with the assumption $\Delta B_n = 0$:

$$F = \frac{x^n + h\gamma}{1 + ahv^n + hd_1}, \; G = \frac{y^n + hax^n v^n}{1 + hcz^n + hd_1 + hb}, \; H = \frac{v^n + hby^n - hh_2 y^n z^n}{1 + hd_1 + hm_1},$$

$$J = \frac{z^n + hcy^n z^n + hh_2 y^n z^n + hm_1 v^n + h\sigma_4 z^n \Delta B_n}{1 + hd_1}.$$

The Jacobian matrix for the system (A9)–(A12) is as follows:

$$J(x, y, v, z) = \begin{bmatrix} \frac{\partial F}{\partial x} & \frac{\partial F}{\partial y} & \frac{\partial F}{\partial v} & \frac{\partial F}{\partial z} \\ \frac{\partial G}{\partial x} & \frac{\partial G}{\partial y} & \frac{\partial G}{\partial v} & \frac{\partial G}{\partial z} \\ \frac{\partial H}{\partial x} & \frac{\partial H}{\partial y} & \frac{\partial H}{\partial v} & \frac{\partial H}{\partial z} \\ \frac{\partial J}{\partial x} & \frac{\partial J}{\partial y} & \frac{\partial J}{\partial v} & \frac{\partial J}{\partial z} \end{bmatrix}.$$

The Jacobian matrix at disease-free equilibrium (DFE) $= D_1 = \left(\frac{r_1}{d_1}, 0, 0, 0\right)$ is as follows:

$$J(D_1) = \begin{vmatrix} \frac{1}{1+hd_1} & 0 & -ha\left(\frac{r_1}{d_1} + hr_1\right) & 0 \\ 0 & \frac{1}{1+hd_1+hb} & \frac{ha\left(\frac{r_1}{d_1}\right)}{1+hd_1+hb} & 0 \\ 0 & \frac{hb}{1+hd_1+hm_1} & \frac{1}{1+hd_1+hm_1} & 0 \\ 0 & 0 & 0 & \frac{1}{1+hd_1} \end{vmatrix},$$

$$|J(D_1) - \lambda| = \begin{vmatrix} \frac{1}{1+hd_1} & 0 & -ha\left(\frac{r_1}{d_1} + hr_1\right) & 0 \\ 0 & \frac{1}{1+hd_1+hb} & \frac{ha\left(\frac{r_1}{d_1}\right)}{1+hd_1+hb} & 0 \\ 0 & \frac{hb}{1+hd_1+hm_1} & \frac{1}{1+hd_1+hm_1} & 0 \\ 0 & 0 & 0 & \frac{1}{1+hd_1} \end{vmatrix},$$

$$\lambda_1 = \left| \frac{1}{1+hd_1} \right| < 1, \lambda_2 = \left| \frac{1}{1+hd_1} \right| < 1,$$

$$|J(D_1)| = \left| \begin{array}{cc} \left(\frac{1}{1+hd_1+hb} \right) & \frac{ha\left(\frac{r_1}{d_1} \right)}{1+hd_1+hb} \\ \frac{hb}{1+hd_1+hm_1} & \frac{1}{1+hd_1+hm_1} \end{array} \right| = 0,$$

$$P_1 = \text{Trace of } J = \left(\frac{1}{1+hd_1+hb} \right) + \frac{1}{1+hd_1+hm_1},$$

$$P_2 = \text{Det of } J = \left(\frac{1}{1+hd_1+hb} \left(\frac{1}{1+hd_1+hm_1} \right) \right) - \left(\frac{ha\left(\frac{r_1}{d_1} \right)}{1+hd_1+hb} \right) \left(\frac{hb}{1+hd_1+hm_1} \right).$$

□

References

1. Tuwairqi, A.; Johani, O.N.A.; Simbawa, A.E. Modeling Dynamics of Cancer Virotherapy with Immune Response. *Adv. Differ. Equ.* **2020**, *438*, 1–26.
2. Crivelli, J.J.; Földes, J.; Kim, P.; Wares, J.R. A mathematical model for cell cycle-specific cancer virotherapy. *J. Biol. Dyn.* **2012**, *6*, 104–120. [CrossRef] [PubMed]
3. Nouni, A.; Hattaf, K.; Yousfi, N. Dynamics of a Virological Model for Cancer Therapy with Innate Immune Response. *Complexity* **2020**, *2020*, 8694821. [CrossRef]
4. Storey, K.M.; Lawler, S.E.; Jackson, T.L. Modeling Oncolytic Viral Therapy, Immune Checkpoint Inhibition, and the Complex Dynamics of Innate and Adaptive Immunity in Glioblastoma Treatment. *Front. Physiol.* **2020**, *11*, 151. [CrossRef] [PubMed]
5. Abernathy, Z.; Abernathy, K.; Stevens, J. A mathematical model for tumor growth and treatment using virotherapy. *AIMS Math.* **2020**, *5*, 4136–4150. [CrossRef]
6. Matos, L.A.; Franco, S.L.; McFadden, G. Oncolytic Viruses and the Immune System: The Dynamic Duo. *Mol. Theory* **2020**, *4*, 349–358.
7. Makaryan, S.Z.; Cess, C.G.; Finley, S.D. Modeling immune cell behavior across scales in cancer. *Wiley Interdiscip. Rev. Syst. Biol. Med.* **2020**, *12*, e1484. [CrossRef]
8. Malinzi, J.; Eladdadi, A.; Sibanda, P. Modelling the spatiotemporal dynamics of chemovirotherapy cancer treatment. *J. Biol. Dyn.* **2017**, *11*, 244–274. [CrossRef]
9. Bajzer, Ž.; Carr, T.; Josić, K.; Russell, S.J.; Dingli, D. Modeling of cancer virotherapy with recombinant measles viruses. *J. Theor. Biol.* **2008**, *252*, 109–122. [CrossRef]
10. Timalsina, S.; Tian, J.P.; Wang, J. Mathematical and Computational Modeling for Tumor Virotherapy with Mediated Immunity. *Bull. Math. Biol.* **2017**, *79*, 1736–1758. [CrossRef]
11. Rommelfanger, D.M.; Offord, C.P.; Dev, J.; Bajzer, Z.; Vile, R.G.; Dingli, D. Dynamics of Melanoma Tumor Therapy with Vesicular Stomatitis Virus: Explaining the Variability in Outcomes Using Mathematical Modeling. *Gene Ther.* **2012**, *19*, 543–549. [CrossRef] [PubMed]
12. Liu, X.; Li, Q.; Pan, J. A deterministic and stochastic model for the system dynamics of tumor–immune responses to chemotherapy. *Phys. A Stat. Mech. Its Appl.* **2018**, *500*, 162–176. [CrossRef]
13. Eftimie, R.; Eftimie, G. Tumour-associated Macrophages and Oncolytic Virotherapies: A mathematical investigation into a complex-dynamics. *Lett. Biomath.* **2018**, *5*, S6–S35. [CrossRef]
14. Santiago, D.N.; Heidbuechel, J.P.W.; Kandell, W.M.; Walker, R.; Djeu, J.; Engeland, C.E.; Abate-Daga, D.; Enderling, H. Fighting Cancer with Mathematics and Viruses. *Viruses* **2017**, *9*, 239. [CrossRef] [PubMed]
15. Kim, S.P.; Lee, P.P. Modeling protective anti-tumor immunity via preventative cancer vaccines using a hybrid agent-based and delay differential equation approach. *PLoS Comput. Biol.* **2012**, *8*, e1002742. [CrossRef]
16. Berg, D.R.; Offord, C.P.; Kemler, I.; Ennis, M.K.; Chang, L.; Paulik, G.; Bajzer, Z.; Neuhauser, C.; Dingli, D. In vitro and in silico multidimensional modeling of oncolytic tumor virotherapy dynamics. *PLoS Comput. Biol.* **2019**, *15*, e1006773. [CrossRef]
17. International Agency for Research on Cancer. Available online: https://gco.iarc.fr/today/data/factsheets/populations/586-pakistan-fact-sheets.pdf (accessed on 1 March 2021).
18. Ijaz, M.F.; Attique, M.; Son, Y. Data-driven cervical cancer prediction model with outlier detection and over-sampling methods. *Sensors* **2020**, *20*, 2809. [CrossRef]
19. Ijaz, M.F.; Alfian, G.; Syafrudin, M.; Rhee, J. Hybrid prediction model for type-2 diabetes and hypertension using DBSCAN-based outlier detection, synthetic minority over-sampling technique (SMOTE), and random forest. *Appl. Sci.* **2018**, *8*, 1325. [CrossRef]
20. Mandal, M.; Singh, P.K.; Ijaz, M.F.; Shafi, J.; Sarkar, R. A tri-stage wrapper-filter feature selection framework for disease classification. *Sensors* **2021**, *21*, 5571. [CrossRef]
21. Panigrahi, R.; Borah, S.; Bhoi, A.K.; Ijaz, M.F.; Pramanik, M.; Kumar, Y.; Jhaveri, R.H. A consolidated decision tree-based intrusion detection system for binary and multiclass imbalanced datasets. *Mathematics* **2021**, *9*, 751. [CrossRef]

22. Panigrahi, R.; Borah, S.; Bhoi, A.K.; Ijaz, M.F.; Pramanik, M.; Jhaveri, R.H.; Chowdhary, C.L. Performance assessment of supervised classifiers for designing intrusion detection systems: A comprehensive review and recommendations for future research. *Mathematics* **2021**, *9*, 690. [CrossRef]

23. Srinivasu, P.N.; SivaSai, J.G.; Ijaz, M.F.; Bhoi, A.K.; Kim, W.; Kang, J.J. Classification of skin disease using deep learning neural networks with mobile net V2 and LSTM. *Sensors* **2021**, *21*, 2852. [CrossRef] [PubMed]

24. Arif, M.S.; Raza, A.; Rafiq, M.; Bibi, M.; Abbasi, J.N.; Nazeer, A.; Javed, U. Numerical Simulations for Stochastic Computer Virus Propagation Model. *Comput. Mater. Contin.* **2020**, *62*, 61–77. [CrossRef]

25. Shatanawi, W.; Arif, M.S.; Raza, A.; Rafiq, M.; Bibi, M.; Abbasi, J.N. Structure-Preserving Dynamics of Stochastic Epidemic Model with the Saturated Incidence Rate. *Comput. Mater. Contin.* **2020**, *64*, 797–811. [CrossRef]

26. Bayram, M.; Partal, T.; Buyukoz, G.O. Numerical methods for simulation of stochastic differential equations. *Adv. Differ. Equ.* **2018**, *2018*, 17. [CrossRef]

27. Abukhaled, M.I.; Allen, E.J. A class of second-order Runge-Kutta methods for numerical solution of stochastic differential equations. *Stoch. Anal. Appl.* **1998**, *16*, 977–991. [CrossRef]

28. Abukhaled, M.; Allen, E.J. A recursive integration method for approximate solution of stochastic differential equations. *Int. J. Comput. Math.* **1998**, *66*, 53–66. [CrossRef]

29. Sghir, A.; Hadiri, S. A new numerical method for 1-D backward stochastic differential equations without using conditional expectations. *Random Oper. Stoch. Equ.* **2020**, *28*, 79–91. [CrossRef]

30. Halidias, N. A novel approach to construct numerical methods for stochastic differential equations. *Numer. Algorithm* **2013**, *66*, 79–87. [CrossRef]

31. Higham, D.J.; Mao, X.; Szpruch, L. Convergence, non-negativity and stability of a new Milstein scheme with applications to finance. *arXiv* **2012**. Available online: https://scholar.google.com/scholar?hl=en&as_sdt=0%2C5&q=Convergence%2C+non-negativity+and+stability+of+a+new+Milstein+scheme+with+applications+to+finance&btnG= (accessed on 1 March 2021).

32. Rebiha, Z. New numerical method for solving nonlinear stochastic integral equations. *Владикавказский Математический Журнал* **2020**, *22*. Available online: https://scholar.google.com/scholar?hl=en&as_sdt=0%2C5&q=New+numerical+method+for+solving+nonlinear+stochastic+integral+equations&btnG= (accessed on 1 March 2021).

33. Słomiński, L. Stability of strong solutions of stochastic differential equations. *Stoch. Process. Their Appl.* **1989**, *31*, 173–202. [CrossRef]

34. Abukhaled, M.I. Mean square stability of second-order weak numerical methods for stochastic differential equations. *Appl. Numer. Math.* **2004**, *48*, 127–134. [CrossRef]